ELSEVIER

Journal of Power Sources 58 (1996) 243–247

JOURNAL OF POWER SOURCES

A study of the degradation of the electrochemical capacity of amorphous $Mg_{50}Ni_{50}$ alloy

Weihong Liu [a,*], Yongquan Lei [b], Dalin Sun [b], Jing Wu [b], Qidong Wang [b]

[a] *Chemistry Department, Fudan University, Shanghai, 200433 People's Republic of China*

[b] *Department of Materials Science and Engineering, Zhejiang University, Hangzhou, 310027 China*

Received 10 January 1996; accepted 29 January 1996

Abstract

The degradation of the electrochemical capacity of amorphous $Mg_{50}Ni_{50}$ alloy during charge-discharge cycling is investigated. The surface morphology and structure of the alloy before and after electrochemical cycling is examined by scanning electron microscopy and X-ray diffraction, respectively. The composition profiles of magnesium, nickel and oxygen are determined by X-ray photoelectron spectroscopy. These results suggest that the capacity deterioration can be attributed to the oxidation of magnesium and nickel in KOH solution during the discharge process, and the reduction of $Ni(OH)_2$ to nickel during the charge process.

Keywords: Magnesium; Nickel; Alloys; Capacity

1. Introduction

Recently, it has been found [1,2] that amorphous $Mg_{50}Ni_{50}$ alloy, synthesized by mechanical alloying, is much easier to activate electrochemically than its crystalline counterpart. It has a maximum capacity of ~500 mAh g^{-1} at a current density of 20 mA g^{-1} on the first cycle. This makes it a very promising electrode material for nickel/metal-hydride secondary batteries. Unfortunately, however, the durability of the amorphous $Mg_{50}Ni_{50}$ alloy is rather poor; it loses almost two-thirds of its discharge capacity after only nine charge/discharge cycles. Such degradation nullifies its practical use as an alloy for electrodes.

In order to clarify the capacity degradation mechanism and, thus, to improve its durability, Lei et al. [1] conducted a study of the structure of the electrode before and after electrochemical cycling by X-ray diffraction (XRD) analysis. It was found that magnesium on the electrode surface had been oxidized to MgO/MgO_2 during cycling and, here by, caused capacity degradation of the electrode alloy. It should be pointed out, however, that the electrode alloy used in that study was mixed with electrolytic copper powder at a weight ratio of 1:2 with the result that the XRD data were concealed by the intense Cu and CuO peaks. In such a situation, it is very surprising that an analysis could be achieved.

In the present study, the phase structure, the composition profiles and the surface morphology of mechanically alloyed, amorphous $Mg_{50}Ni_{50}$ alloy are examined in detail before and after electrochemical cycling. An explanation for the capacity degradation is derived.

2. Experimental

The $Mg_{50}Ni_{50}$ alloy was synthesized by mechanical alloying (MA) the pure metal powders at the designed composition. To prevent the alloy from being oxidized during milling, the powder mixture was sealed under argon in a tightly-closed steel vial. The mechanical alloying was performed with a ball to powder weight ratio of 15:1. To avoid a large temperature rise of the mixture, a intermittent working procedure was employed. The milling was performed for 120 h.

The alloy synthesized by MA was cold pressed, under a pressure of 400 kg cm^{-2}, into electrode pellets of 10 mm diameter and 3 mm thickness for electrochemical testing. The electrochemical cycling was performed in a conventional three-plate system with 6 M KOH solution. A nickel electrode ($Ni(OH)_2/NiOOH$) was used as the counter electrode and a mercury/mecurous oxide electrode (Hg/HgO, 6 M KOH) was used as the reference electrode. Charging was conducted at a current density of 40 mA g^{-1} for 20 h. Discharging was performed at a current density of 100 mA g^{-1} at atomspheric pressure and room temperature. The end-of-discharge poten-

* Corresponding author.

PII S0378-7753(96)02394-1

tial was fixed at −600 mV (versus Hg/HgO, 6M KOH). After 4 or 9 charge/discharge cycles, the electrode pellet was washed with distilled water to remove the K^+ and OH^- ions, and then dried in an air current at 353 K.

X-ray diffraction (XRD), X-ray photoelectron spectroscopy (XPS) and scanning electron microscopy (SEM) analysis were performed on a D/Max- II B X-ray diffractometer, an ESCALAB MK III X-ray photoelectron spectrometer and a S-570 scanning electron microscometer with a microprobe analyser, respectively.

3. Results and discussion

3.1. X-ray diffraction

The XRD patterns of $Mg_{50}Ni_{50}$ amorphous alloy, before and after electrochemical cycling, are shown in Fig. 1. The XRD pattern recorded immediately after MA displays a diffused maximum that is typical of an amorphous phase. The amorphous structure of MA $Mg_{50}Ni_{50}$ alloy was further confirmed by the results of TEM and DSC analysis [3]. After four cycles, some small sharp peaks appeared. These were superimposed on the broad amorphous maximum at the positions of crystalline $Mg(OH)_2$ and nickel. This implies that the amorphous structure of the electrode alloy is stable during charge/discharge cycling, but that the powder surface (especially the magnesium component) is oxidized severely in KOH solution. In contrast to the results of Lei et al. [1], the surface oxidization product is mainly $Mg(OH)_2$ and nickel, as opposed to of MgO/MgO_2, as can be seen in Fig. 1. The distinct peaks at the position of $Mg(OH)_2$ (001), (101), (102), (110), (111) and Ni (111) indicate the presence of $Mg(OH)_2$ and nickel.

3.2. X-ray photoelectron spectroscopy

The Mg(2p) spectra for air-exposed $Mg_{50}Ni_{50}$ taken immediately after machanical alloying and after four charge/discharge cycles are given in Figs. 2 and 3, respectively. The results indicate that magnesium loses its metallic state after cycling and that all the magnesium on the surface of the electrode is oxidized. The position of the Mg(2p) peak agrees well with the spectra for oxidized magnesium, according to which the 2p levels of magnesium are shifted by about 0.9 eV to the high binding energy (BE) side of metallic magnesium. The Mg(2p) spectra for the $Mg_{50}Ni_{50}$ electrode pellet taken immediately after nine cycles and after different sputtering periodes are presented in Fig. 3. The electrochemical cycling shifts the Mg(2p) level by 0.8 eV away from metallic magnesium to the higher BE side; this indicates the formation of $Mg(OH)_2$. The shapes of these lines are characteristic of a partly resolved doublet (a shoulder on the high BE side) spaced 1.0 eV apart. The latter is assigned to a hydroxide, namely, $Mg(OH)_2$. Upon sputtering, the gradual appearance of the metallic magnesium peak and the disap-

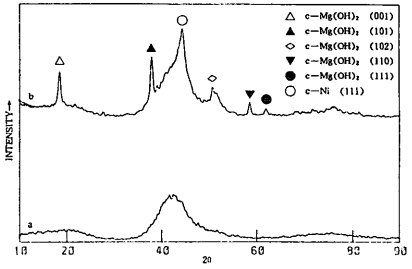

Fig. 1. XRD pattern of $Mg_{50}Ni_{50}$: (a) immediately after mechanical alloying; (b) after 4 charge/discharge cycles.

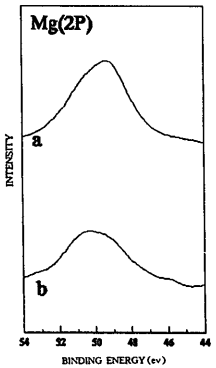

Fig. 2. XPS spectra Mg(2p) of amorphous $Mg_{50}Ni_{50}$: (a) immediately after mechanical alloying; (b) after 4 charge/discharge cycles.

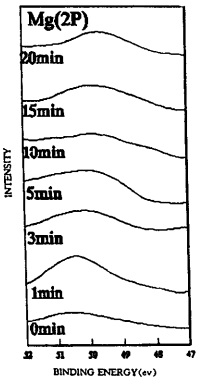

Fig. 3. XPS spectra Mg(2p) of air-exposed and sputtered $Mg_{50}Ni_{50}$ electrode pellet after 9 cycles.

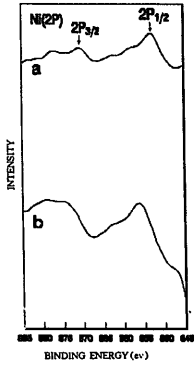

Fig. 4. XPS spectra Ni (2p) of air-exposed amorphous $Mg_{50}Ni_{50}$: (a) immediately after mechanical alloying; (b) after 4 charge/discharge cycles.

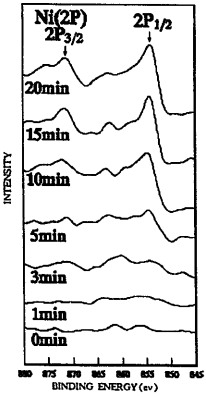

Fig. 5. XPS spectra Ni (2p) of air-exposed and sputtered $Mg_{50}Ni_{50}$ electrode pellet after 9 cycles.

pearance of the surface $Mg(OH)_2$ is observed, though the oxide layers are of considerable thickness, as can be seen from Fig. 3.

The Ni(2p) spectra for the air-exposed $Mg_{50}Ni_{50}$ taken immediately after mechanical alloying and after four cycles are given in Fig. 4. The charge/discharge cycling of $Mg_{50}Ni_{50}$ in KOH solution shifts the Ni(2p) level by 3.7 eV away from metallic nickel (Fig. 4). This suggests the formation of Ni^{2+} and, thus, contradicts the results of XRD analysis. The formation of $Ni(OH)_2$ can be definitely derived from the measured energies in the Ni(2p) spectrum and from the characteristic pattern change with the main peak, a separation of 7.0 eV [4]. The oxidation of nickel during discharge was also observed by Zuttel et al. [5]. The Ni(2p) spectra for the $Mg_{50}Ni_{50}$ electrode pellet taken immediately after nine cycles and after different sputtering periods are shown in Fig. 5. The nickel present on the surface was largely in the oxidized form, as deduced from its BE of $2p_{(3/2)}$-level, which is about 3.5 eV away from metallic nickel. Upon sputtering, $Ni(OH)_2$ disappeared and a pronounced increase of metallic nickel was seen. The concentration of nickel oxide was relatively small compared with that of $Mg(OH)_2$ and metallic nickel present on the surface. We conclude that the low concentration prevented the appearance of lines of nickel oxide in the XRD pattern.

3.3. Electrochemical potential analysis

The charge/discharge reactions at the hydrogen storage negative electrode are as follows:

(i) charge:

$$M + H_2O + e^- \rightarrow MH + OH^- \quad (1)$$

(ii) discharge:

$$MH + OH^- \rightarrow M + H_2O + e^- \quad (2)$$

and the equilibrium potentials for some electrode reactions are listed in Table 1 [6].

It is well accepted that the reduction of high-valence metal ions to metallic elements can occur only at a potential less than the Φ value listed in Table 1. The potential difference between a metal element in the anode alloy and its equilibrium reaction potential reflects the oxidation driving force of the electrode reaction.

During charge/discharge cycling, the electrode potential of the hydrogen storage electrode is in the range −0.93 to −0.60 V versus Hg/HgO. Therefore, the magnesium element in the alloy should be in the oxidized state, Mg^{2+}, and the tendency to form $Mg(OH)_2$ is much higher than that of MgO. The electrode potential of the hydrogen storage anode differs from the equilibrium potential of the electrode reaction C in Table 1. Thus, oxidation of nickel to $Ni(OH)_2$, and reduction of $Ni(OH)_2$ to nickel, occurs during charge/discharge cycling. The maximum oxidation driving force of nickel is $\Delta\Phi_{max} = 0.09$ V, i.e., quite low. Therefore, the degree of oxidation of nickel during cycling is quite limited and the hydroxide, $Ni(OH)_2$, formed can be easily reduced to metallic nickel in the subsequent charging process.

Table 1
Equilibrium potentials of electrode reactions [6]

	Electrode reaction	Equilibrium potential (V)	
		Φ	Φ vs. Hg/HgO
A	$Mg(OH)_2 + 2e^- \leftrightarrows Mg + 2OH^-$	−2.68	−2.778
B	$Mg^{2+} + 2e^- \leftrightarrows Mg$	−2.34	−2.438
C	$Ni(OH)_2 + 2e^- \leftrightarrows Ni + 2OH^-$	−0.69	−0.788
D	$Ni^{2+} + 2e^- \leftrightarrows Ni$	−0.250	−0.348
E	$HgO + H_2O + 2e^- \leftrightarrows Hg + 2OH^-$	0.098	0

Based on the experimental facts, we conclude that the oxidation (degradation) and reduction reactions of the negative electrode during cycling are:

(i) discharge:

$$Mg + 2OH^- \rightarrow Mg(OH)_2 + 2e^- \quad (3)$$

$$Ni + 2OH^- \rightarrow Ni(OH)_2 + 2e^- \quad (4)$$

(ii) charge:

$$Ni(OH)_2 + 2e^- \rightarrow Ni + 2OH^- \quad (5)$$

Thus, the easily reducible nickel hydroxide generated during discharge is reduced to nickel during the subsequent charging procedure and the amount of nickel increases with cycling under the experimental conditions. As a result, the nickel hydroxide generated during cycling is limited, yet the amount of nickel increases with cycling. Thus, the oxidation of magnesium causes the decomposition of amorphous $Mg_{50}Ni_{50}$ alloy into $Mg(OH)_2$ and nickel at the powder surface and interface. Accordingly, the final electrode alloy after cycling reveals a much higher degree of oxidation of magnesium than nickel and has larger amounts of $Mg(OH)_2$ and nickel than $Ni(OH)_2$ on the alloy surface, and the weight ratios of $Mg(OH)_2$ to $Ni(OH)_2$ and nickel to $Ni(OH)_2$ both increase with cycling.

3.4. Scanning electron microscopy

The particles of the amorphous alloy synthesized by mechanical alloying are spherical grains with large interfaces and defects, as shown in Fig. 6(a). The grain size varies between 3 and 20 μm in diameter. The particles have high specific surface area.

An electron micrograph of the amorphous particles after four cycle is shown in Fig. 6(b). It can be seen that a white and loose surface layer is formed on the grey amorphous particle matrix, and that the particle surface becomes smoother on cycling. On the basis of the above XRD and XPS results, it is concluded that this white zone is a surface oxidation layer.

A clear view of the surface oxidation procedure of the amorphous Mg–Ni particles in alkaline KOH solution during cycling can be derived from the above observations. During each discharge, both magnesium and nickel on the active alloy surface are oxidized, yet, virtually all the easily reducible nickel oxide is reduced to metal nickel during the subsequent charging procedure. Thus, the total oxidation rate of magnesium is much faster than that of nickel. Moreover, the degree of oxidation is much higher. The final powder surface contains some $Ni(OH)_2$ and greater amounts of $Mg(OH)_2$ and nickel.

It is known [7] that the surface hydroxides of magnesium and nickel both inhibit the dissociative adsorption of hydrogen and the transfer of hydrogen from the surface to bulk, and such surface layers also inhibit dehydriding reversibly. Thus, the alloy activity is lowered. Moreover, the oxidation

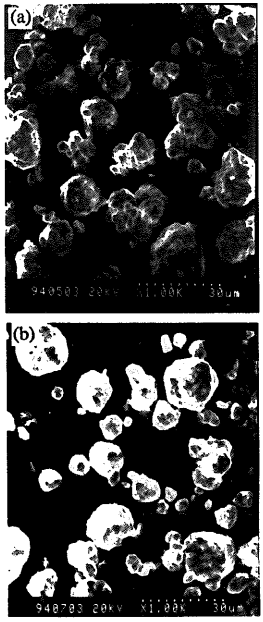

Fig. 6. SEM of amorphous $Mg_{50}Ni_{50}$: (a) immediately after mechanical alloying; (b) after 4 charge/discharge cycles.

of magnesium results in the growth of non-reducible $Mg(OH)_2$ and causes loss of the hydrogen-absorbing element in the alloy and thus decreases its hydrogen-storage ability. Further, the oxidation of magnesium and nickel degrades the grain-to-grain contact and causes an increase in the internal resistance of the electrode. Therefore, the charge/discharge capacity of the electrode declines during cycling.

4. Conclusions

The deterioration in the capacity of amorphous $Mg_{50}Ni_{50}$ alloy synthesized by mechanical alloying is attributed to the oxidation of magnesium and nickel during cycling in KOH solution. The amorphous $Mg_{50}Ni_{50}$ alloy is oxidized on the surface to form $Ni(OH)_2$ and larger amounts of $Mg(OH)_2$ and nickel during electrochemical cycling. Surface oxidation may effect the electrical conductivity of the electrode. The oxidization of Mg causes a loss of the hydrogen-storage element and the Mg $(OH)_2$ is non-reducible and inhibits both the hydrogen dissociation process and the transfer of hydrogen atoms. The nickel hydroxide $Ni(OH)_2$ formed during discharging also inhibits the hydriding and dehydriding processes, yet, it can be reduced to active nickel during the sub-

sequent charging process. Thus, the level of magnisium oxidation is much higher than that of nickel.

References

[1] Y.Q. Lei, Y.M. Wu, Q.M. Yang, J. Wu and Q.D. Wang, *Z. Phys. Chem., 183* (1994) 379–384.
[2] Q.M. Yang, Y.Q. Lei, C.P. Chen, J. Wu and Q.D. Wang, *J. Mater. Sci. Technol.*, 9 (1993) 125–128.
[3] W.H. Liu, Y.Q. Lei, J. Wu and Q.D. Wang, to be published.
[4] P. Selvam, B. Viswanathan and V. Srinivasan, *J. Less- Common Met., 158* (1990) L1–L7.
[5] A. Zuttel, F. Meli and L. Schlapbach, *J. Alloys Comp., 226* (1994) 31–38.
[6] Y.F. Liu, *Techniques of Electrochemistry*, 1987.
[7] P. Selvam, B. Viswanathan, C.S. Swamy and V. Srinivasan, *Int. J. Hydrogen Energy, 11* (1986) 169–192.